

# Modulation of a Pre-existing Conformational Equilibrium Tunes Adenylate Kinase Activity

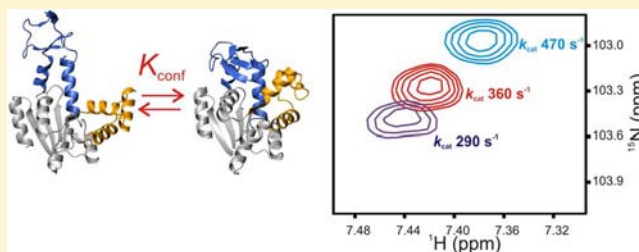
Jörgen Ådén,<sup>†</sup> Abhinav Verma,<sup>‡</sup> Alexander Schug,<sup>‡</sup> and Magnus Wolf-Watz<sup>\*†</sup>

<sup>†</sup>Department of Chemistry, Chemical Biological Center, Umeå University, SE-901 87 Umeå, Sweden

<sup>‡</sup>Steinbuch Centre for Computing, Karlsruhe Institute of Technology, 76131 Karlsruhe, Germany

**S** Supporting Information

**ABSTRACT:** Structural plasticity is often required for distinct microscopic steps during enzymatic reaction cycles. Adenylate kinase from *Escherichia coli* (AK<sub>eco</sub>) populates two major conformations in solution; the open (inactive) and closed (active) state, and the overall turnover rate is inversely proportional to the lifetime of the active conformation. Therefore, structural plasticity is intimately coupled to enzymatic turnover in AK<sub>eco</sub>. Here, we probe the open to closed conformational equilibrium in the absence of bound substrate with NMR spectroscopy and molecular dynamics simulations. The conformational equilibrium in absence of substrate and, in turn, the turnover number can be modulated with mutational- and osmolyte-driven perturbations. Removal of one hydrogen bond between the ATP and AMP binding subdomains results in a population shift toward the open conformation and a resulting increase of  $k_{\text{cat}}$ . Addition of the osmolyte TMAO to AK<sub>eco</sub> results in population shift toward the closed conformation and a significant reduction of  $k_{\text{cat}}$ . The Michaelis constants ( $K_M$ ) scale with the change in  $k_{\text{cat}}$ , which follows from the influence of the population of the closed conformation for substrate binding affinity. Hence,  $k_{\text{cat}}$  and  $K_M$  are mutually dependent, and in the case of AK<sub>eco</sub>, any perturbation that modulates  $k_{\text{cat}}$  is mirrored with a proportional response in  $K_M$ . Thus, our results demonstrate that the equilibrium constant of a pre-existing conformational equilibrium directly affects enzymatic catalysis. From an evolutionary perspective, our findings suggest that, for AK<sub>eco</sub>, there exists ample flexibility to obtain a specificity constant ( $k_{\text{cat}}/K_M$ ) that commensurate with the exerted cellular selective pressure.



## INTRODUCTION

Enzymes are extraordinary biocatalysts that can increase the rate of chemical reactions several orders of magnitude, making chemical reactions to occur on a time scale that is compatible with global biological processes such as cell division. For instance, the rate enhancement of orotidine 5'-phosphate decarboxylase is estimated to be 10<sup>17</sup>-fold.<sup>1</sup> Many of the microscopic steps during enzymatic reaction cycles are dependent on structural plasticity (or conformational dynamics) of the biocatalyst itself. It has been shown for several enzymes including dihydrofolate reductase,<sup>2</sup> RNase A,<sup>3</sup> cyclophilin A<sup>4</sup> and *Escherichia coli* adenylate kinase (AK<sub>eco</sub>)<sup>5,6</sup> that conformational dynamics, in fact, can represent the rate-limiting microscopic step for catalytic turnover. The enzymes described above display what is referred to as pre-existing equilibria where the substrate-free states are in equilibrium with “substrate bound-like” structures that are only scarcely populated. In the conformational selection model,<sup>7</sup> these bound-like structures harbor the substrate binding activity. To deepen the current knowledge of enzymatic catalysis, it is crucial to understand the molecular details that influence conformational dynamics, and how conformational dynamics affects catalysis. AK<sub>eco</sub> is an excellent model system in studies of the linkage between dynamics and enzymatic catalysis since its function is dependent on large-scale conformational changes (Figure 1).

AK<sub>eco</sub> catalyzes the magnesium-dependent reversible interconversion of AMP and ATP into two ADP molecules and harbors distinct ATP and AMP binding subdomains (ATPlid and AMPbd). The global stability of the enzyme is governed by the CORE subdomain.<sup>8,9</sup> The enzyme primarily populates two distinct conformations in solution: the open<sup>10</sup> (inactive) and the closed (active) states.<sup>11,12</sup> Interconversion between these states is associated with large conformational rearrangements of the ATPlid and AMPbd (Figure 1A,B), and the rate of opening of the substrate binding subdomains (or alternatively expressed the inverse of the lifetime of the closed state ( $\tau_c$ )) in the presence of bound substrate is rate-limiting for catalysis (Figure 1D).<sup>5,6</sup> Since the definition of  $k_{\text{cat}}$  is the rate-limiting microscopic step for breakdown of the ES complex and generation of product,<sup>13</sup> the rate constant of subdomain opening in AK<sub>eco</sub> is equal to  $k_{\text{cat}}$ . The molecular mechanism of ATPlid closure follows an “order to disorder”<sup>14</sup> or “cracking”<sup>15</sup> mechanism where specific helical segments in the ATPlid unfold with subsequent refolding into the closed conformation.

Closed-like AK<sub>eco</sub> conformations are populated already in the absence of substrate,<sup>6,12,17</sup> and addition of substrates

Received: April 4, 2012

Published: September 10, 2012

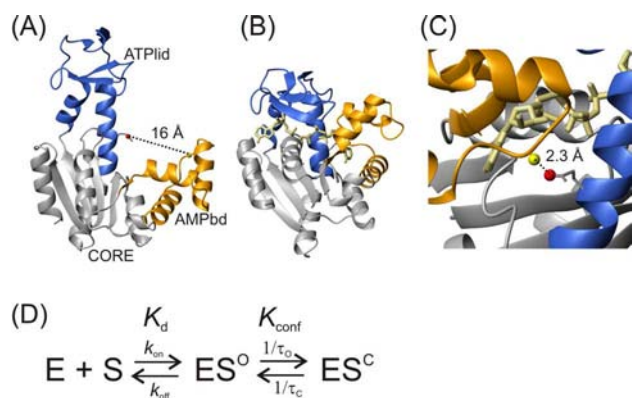


**Figure 1.** Stabilization of the closed  $AK_{eco}$  conformation with an interdomain hydrogen bond suggested from the crystal structure. (A) Crystal structure of substrate free open  $AK_{eco}$ .<sup>10</sup> The distance between the Glu170 side chain hydrogen bond acceptor ( $O^\delta$  atom, red sphere) and the Leu58 backbone amide hydrogen bond donor (yellow sphere) is 16 Å in open  $AK_{eco}$ . The ATPlid, AMPbd, and CORE subdomains are indicated and colored blue, yellow, and gray, respectively. (B) Structure of closed  $AK_{eco}$ <sup>11</sup> in presence of the tight binding inhibitor Ap5A (khaki). (C) The closed  $AK_{eco}$  conformation is stabilized with a hydrogen bond between Glu170 and Leu58; the distance (2.3 Å) between hydrogen bond donor and acceptor is indicated in an expanded and rotated view with respect to (B). The molecular graphics images were generated with MolMol.<sup>16</sup> (D) Nucleotide binding mechanism for  $AK_{eco}$ . E corresponds to enzyme, S to substrate,  $ES^O$  to a transient substrate bound equilibrium complex and  $ES^C$  to the active conformation of  $AK_{eco}$ . The superscripts “O” and “C” refer to  $AK_{eco}$  in open (inactive) and closed (active) conformations. The equilibrium constants for the initial binding event and the following conformational changes are given by  $K_d$  and  $K_{conf}$ , respectively. See the Supporting Information for a detailed description of  $K_{conf}$ . The lifetimes of open and closed states are equal to  $\tau_o$  and  $\tau_c$ , respectively, under substrate saturating conditions.

redistribute pre-existing states by stabilizing the closed conformation.<sup>12</sup> Hence, in  $AK_{eco}$ , the same dynamic event (i.e., opening/closing) occurs in both substrate free and substrate bound states. Sophisticated fluorescence techniques can provide detailed single-molecule insight about conformational dynamics, but require labeling of specific sites.<sup>18</sup> Solution state NMR spectroscopy provides label-free approaches to quantify conformational dynamics in proteins with residue-specific resolution. In particular, relaxation dispersion experiments<sup>19,20</sup> can provide information on the structure,<sup>21</sup> thermodynamics and kinetics of exchange processes in proteins. The most readily accessible and accurate parameter in NMR spectroscopy is the chemical shift. Recent developments have shown that chemical shifts can be used to determine high-resolution protein structures<sup>22–24</sup> but also to quantify conformational dynamics<sup>12,25–28</sup> and allostery<sup>29</sup> in proteins. Here, we show that the open/closed  $AK_{eco}$  equilibrium can be modulated in opposite directions by either removal of one interdomain hydrogen bond distant from the active site or by addition of the osmolyte TMAO. Remarkably, modulation of closed state populations is propagated to proportional responses in the catalytic parameters  $k_{cat}$  and  $K_M$  of  $AK_{eco}$ .

## MATERIALS AND METHODS

**Protein Purification and Mutagenesis.** Both wild-type and E170A  $AK_{eco}$  were expressed and purified as described previously.<sup>5</sup> Protein concentrations were quantified by measuring the absorption at 280 nm using an extinction coefficient of  $10.430 \text{ M}^{-1} \text{ cm}^{-1}$ . Site-

directed mutagenesis was performed with the Quickchange approach (Stratagene) with oligonucleotide primers purchased from Eurofins MWG Operon. The E170A mutation was verified with DNA sequencing (Eurofins MWG Operon).

**Circular Dichroism.** Far ultraviolet CD experiments were performed on a Jasco J-810 spectropolarimeter. Thermal unfolding was followed by monitoring the CD signal at 220 nm in a 1 mm cuvette and a scan rate of  $1 \text{ deg min}^{-1}$ . Protein concentrations in the CD experiments were  $7.5 \mu\text{M}$  in a buffer consisting of 10 mM sodium phosphate and 50 mM NaCl at pH 7.0. Melting temperatures were quantified with nonlinear fits (Microcal Origin) of CD-data to a two-state transition.<sup>30</sup>

**Enzymatic Assays.** Enzyme activity in the direction of ADP formation at  $25^\circ\text{C}$  was quantified with a coupled ATPase assay.<sup>31</sup> All reagents for the assay were purchased from Sigma-Aldrich. Catalytic parameters were obtained through fits of initial velocities to the Michaelis–Menten equation. In all conditions, care was taken to ensure that the amount of coupling enzymes (pyruvate kinase and lactate dehydrogenase) was not limiting the reactions.  $AK_{eco}$  concentrations were calculated by measurements in triplicate.

**NMR Spectroscopy.** All NMR experiments were acquired on a Bruker DRX 600 MHz spectrometer equipped with a 5-mm triple resonance z-gradient cryoprobe. The temperature in all NMR experiments was  $25^\circ\text{C}$ . Temperature calibration was accomplished with a temperature probe inserted into the sample compartment of the cryoprobe. The NMR sample buffer was 30 mM MOPS pH 7.0 and 50 mM NaCl with 10% (v/v)  $^2\text{H}_2\text{O}$ . Protein concentrations ranged between 600 and 900  $\mu\text{M}$  supplemented with 2.5 mM Ap5A (Sigma-Aldrich) in case of analysis of closed states. Assignments of E170A in apo and Ap5A saturated states were accomplished with 3D  $^{15}\text{N}$  NOESY-HSQC experiments using a pulse sequence from the Bruker library. Hydrogen to deuterium exchange experiments were performed as described in Rundqvist et al.<sup>8</sup> NMR spectra were processed with NMRPipe<sup>32</sup> and visualized in Ansig for Windows.<sup>33</sup>

**Molecular Dynamics Simulation.** Molecular dynamics simulations were performed using Amber99sb-ildn 8<sup>34</sup> with explicit TIP3P 9<sup>35</sup> solvent on the crystal structure 1AKE.PDB<sup>11</sup> and sodium counterions to neutralize the system (12 Å solvation shell, cubic box of 77.5 Å with periodic boundary conditions, approximately 47 000 atoms) for  $3 \times 1 \mu\text{s}$  stochastic dynamics (time step of 2 fs), and Particle Mesh Ewald electrostatics. We stress the necessity of the large solvation shell to prevent  $AK_{eco}$  self-interactions with its periodic images due to conformational motions. Langevin temperature coupling (300 K, inverse friction constant 0.1 ps) and Berendsen pressure coupling was employed. All simulations are run in Gromacs<sup>36</sup> v4.5.4. To calculate water mediation of hydrogen bonds, only water molecules in the region of 6 Å surrounding the NH of Leu58 and  $O^\delta$  of E170 are considered. All possible hydrogen bonds between L58, E170 and selected waters are calculated using PyMOL using the methodology of DSSP<sup>37</sup> and the shortest possible distance (in molecules) between L58 and E170 is recorded.

## RESULTS AND DISCUSSION

**Mutational Induced Perturbation of  $AK_{eco}$ .** The closed  $AK_{eco}$  conformation is stabilized with an interdomain hydrogen bond suggested from the crystal structure (1AKE.pdb). This hydrogen bond is donated from the amide hydrogen ( $H^N$ ) of Leu58 in AMPbd to the  $O^\delta$  side chain oxygens of Glu170 in the ATPlid (Figure 1C). This interaction has been suggested to partially explain the cooperative closure of both substrate binding domains in response to simultaneous binding of ATP and AMP.<sup>12</sup> The hydrogen bond is only present in the closed state (the distance between donor and acceptor in the open state is 16 Å Figure 1A), and is thus expected to affect the open/closed conformational equilibrium. NMR detected hydrogen to deuterium exchange experiments<sup>8</sup> were used to indirectly observe formation of this important hydrogen bond in closed  $AK_{eco}$  in solution (Figure 2). There exist small

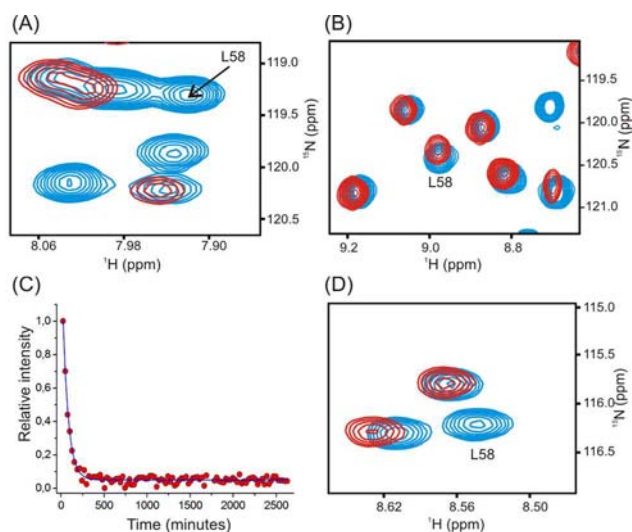


**Figure 2.** Indirect observation of the E170-L58 hydrogen bond in closed wild-type  $AK_{eco}$ . Shown are  $^1H-^{15}N$  HSQC expansions representing protonated reference spectra (blue contours) and the first spectra after exchange of protonated  $AK_{eco}$  into  $^2H_2O$  (red contours). The position of the NH correlation for Leu58 is indicated in all panels. (A) apo  $AK_{eco}$  (open state). (B)  $AK_{eco}$  in complex with Ap5A (closed state). (C) Hydrogen to deuterium exchange kinetics for the Leu58 amide proton in the closed Ap5A complex, the best fitted single exponential decay is shown as a blue line. (D) E170A in complex with Ap5A (closed state).

chemical shift differences between the experiments performed in  $^1H_2O$  and  $^2H_2O$ , these differences are likely dependent on minute differences in pH values in the samples. In apo  $AK_{eco}$ , the hydrogen bond to the  $H^N$  atom of Leu58 is not present in the crystal structure, and consequently the amide hydrogen of Leu58 exchanges within the dead-time of the experiment (11 min) (Figure 2A). In contrast, this hydrogen atom shows substantial protection toward exchange in the closed Ap5A bound state (Figure 2b). Protection against deuterium exchange is generally considered as indirect evidence of hydrogen bonds.<sup>38</sup> Evaluation of exchange kinetics (using the formalism described in ref 39) reveals that the local free energy for the hydrogen bond is  $16 \text{ kJ mol}^{-1}$  (Figure 2C) (see Supporting Information and BMRB entry 18685). The calculation assumes that the exchange occurs in the EX2 regime which previously has been shown for residues in the AMPbd of  $AK_{eco}$ .<sup>8</sup> Since the  $H^N$  hydrogen atom of Leu58 is fully exposed to the solvent in the open state, a lower bound of the free energy difference between open and closed states in the Ap5A bound complex can be estimated from the stability of the hydrogen bond. The free energy difference corresponds to an open/closed equilibrium constant ( $K_{conf}$  in Figure 1D, see the Supporting Information for a description of  $K_{conf}$ ) equal to  $\sim 700$  in the direction of domain closure. This value should be compared to the  $K_{conf}$  value for ATP binding which is equal to 1.5.<sup>12</sup> By combining the apparent binding constant for Ap5A to  $AK_{eco}$  ( $0.14 \mu\text{M}^{14}$ ) with the minimal reaction scheme (Figure 1D) for Ap5A binding and  $K_{conf}$  equal to 700, the dissociation constant ( $K_d$  in Figure 1D) for Ap5A was found to be  $100 \mu\text{M}$ . Hence, the effect of the conformational change in  $AK_{eco}$  with respect to Ap5A binding is to increase the binding affinity almost 3 orders of magnitude ( $100/0.14$ ). The ATP mimicking part of Ap5A is sandwiched between residues in the ATPlid and CORE subdomains (Figure 1B). Hence, Ap5A is bound with

two interaction interfaces, both of which must be in contact with Ap5A for  $AK_{eco}$  to utilize fully the binding energy.  $K_{conf}$  describes to which extent both interaction interfaces are engaged in Ap5A binding once the initial Ap5A: $AK_{eco}$  complex has been formed.

To access the importance of the interdomain hydrogen bond, Glu170 was mutated into alanine (E170A) which eliminates the capacity of the side-chain at residue 170 to accept a hydrogen bond. E170A is a well folded protein based on the chemical shift dispersion and narrow distribution of peak intensities in a  $^1H-^{15}N$  HSQC spectrum (Supporting Information Figure S1A). On a global scale the chemical shift perturbations in E170A referenced to the wild type are small (Supporting Information Figure S1B) showing that the structural perturbation of the mutant is minimal and that open ground states are very similar in mutant and wild type. There, however, exist small but significant differences in chemical shifts for a limited set of residues and these differences carry important information on ATPlid dynamics. Figure 3A shows a structural

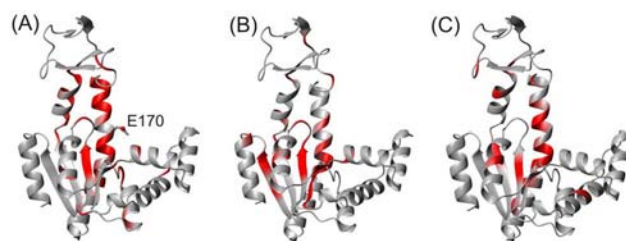


**Figure 3.** Chemical shift perturbations in E170A and TMAO perturbed  $AK_{eco}$ . Significant chemical shifts (Supporting Information Figure S1B,C) in E170A (A) and in  $AK_{eco}$  with 0.35 M TMAO (B) are displayed in red on open  $AK_{eco}$ . The  $O^\epsilon 1$  atom of Glu170 is shown as a red sphere on its side chain in panel (A). Chemical shift perturbations are referenced to wild type  $AK_{eco}$  according to:  $\delta\omega = 0.2|\delta^{15}N| + |\delta^1H|$  (ppm). (C) Residues that show significant chemical shift perturbations in response to ATP binding (adapted from ref 12).

display of the chemical shift perturbations in E170 compared to wild-type  $AK_{eco}$ . The differences are clustered at positions that are known to respond to ATPlid dynamics (Figure 3C).<sup>12</sup> Hydrogen to deuterium exchange experiments suggest that the hydrogen bond donated by Leu58 is absent in both open (not shown) and closed E170A conformations (Figure 2D).

The surface exposed mutation does not significantly influence the stability of either apo (open) or Ap5A bound (closed) states as evidenced by marginal ( $\sim 0.7 \text{ }^\circ\text{C}$ ) reduction of melting temperatures ( $T_m$ ) compared to wild-type  $AK_{eco}$  (Table 1 and Figure 4A,B). Taken together, the NMR and stability measurements suggest that, overall, the open and

**Table 1. Thermal Stabilities of  $AK_{eco}$  and E170A**

protein	apo ( $T_m$ , $^\circ\text{C}$ )	Ap5A <sup>a</sup> ( $T_m$ , $^\circ\text{C}$ )
WT	$57.0 \pm 0.2^b$	$64.5 \pm 0.2$
WT + 0.35 M TMAO	$56.9 \pm 0.2$	$65.9 \pm 0.2$
E170A	$56.3 \pm 0.2$	$63.9 \pm 0.2$
E170A + 0.35 M TMAO	$55.7 \pm 0.2$	$66.5 \pm 0.2$

<sup>a</sup>The Ap5A concentration was  $400 \mu\text{M}$  (further increase in the concentration did not result in increased  $T_m$  values). <sup>b</sup>Errors are estimated from repeat measurements, the error from the nonlinear fitting routine is around  $0.02 \text{ }^\circ\text{C}$ .

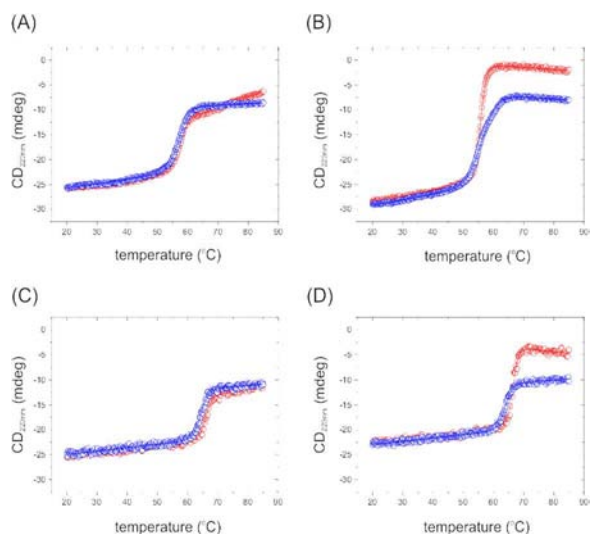


**Figure 4.** Thermal stabilities of wild-type and E170A  $AK_{eco}$ . Thermal stabilities were quantified by following the CD signal at 220 nm as a function of temperature. Melting points ( $T_m$ ) were quantified by fits of the data to a two state transition (solid lines). The thermal transitions are 60–90% reversible. In all panels, blue circles corresponds to regular buffer and red circles corresponds to buffer supplemented with 0.35 M TMAO. (A) apo  $AK_{eco}$ ; (B) apo E170A; (C)  $AK_{eco}$  with Ap5A; (D) E170A with Ap5A.

closed structural basins in wild-type and E170A  $AK_{eco}$  are very similar but that ATPid dynamics is affected.

Inspired by the presence of the L58/E170 hydrogen bond in closed  $AK_{eco}$ , we performed three 1  $\mu$ s unrestrained molecular dynamics (MD) simulations with explicit solvent to probe the initial events during subdomain opening. Other simulation studies have focused on the open to closed transition<sup>40–42</sup> and also at estimation of the free energy difference between open and closed states.<sup>43,44</sup> Since this report (see below) and other studies<sup>6,12,17</sup> have shown that  $AK_{eco}$  samples closed-like conformation in absence of substrate, the simulations were initiated from closed substrate-free  $AK_{eco}$  with the L58/E170 hydrogen bond intact. Overall, the three simulations capture the closed to open transition albeit to different extent. In the first simulation,  $AK_{eco}$  remains in the closed state for almost 1  $\mu$ s and starts to open toward the end of the simulation (Figure 5A). The other two simulations sample the opening event within 0.1  $\mu$ s (see Supporting Information Figure S2). In all simulations, a fast relaxation process that corresponds to a slight opening of the ATPid is observed within the first 20 ps. During this event, the direct hydrogen bond between L58 and E170 is substituted by an indirect hydrogen bond as one or two water molecules (Figure 5) enter and satisfy the hydrogen bonding acceptor and donor capabilities of positions 170 and 58. Hence, breathing within the closed structural basin is accompanied by accommodation of one or two water molecules that bridge the hydrogen bond between positions 58 and 170. Still, the presence of early water molecules in MD simulations should be treated with caution. While MD simulations stimulate understanding of the dynamics of water hydrogen bond networks in biomolecular systems<sup>45</sup> and significant effort has been spent on investigating the role of water mediation,<sup>46</sup> concerns have been raised that force field artifacts can influence hydrogen bonding.<sup>47</sup> On the other hand, it is interesting that in the crystal structure of closed  $AK_{eco}$  (1AKE.PDB) there is no water molecule bridging this hydrogen bond. This can in

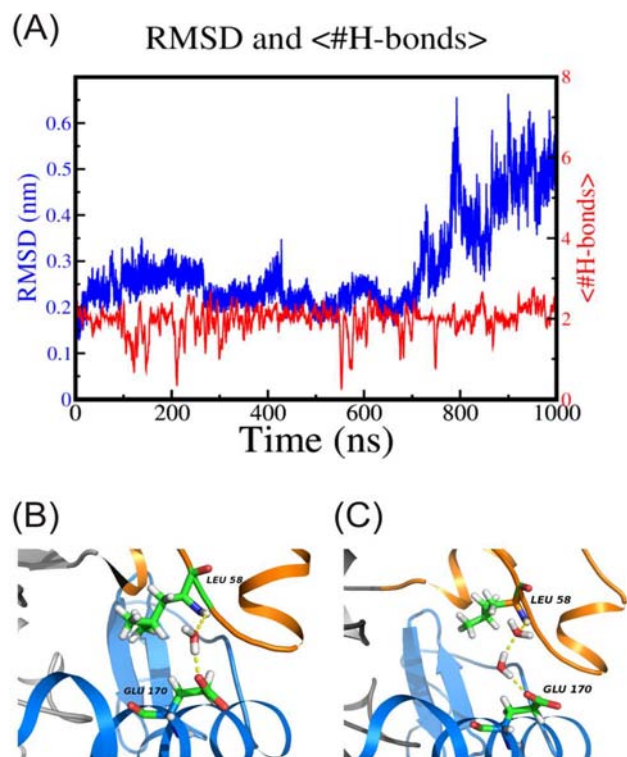


**Figure 5.** Water-mediated L58/E170 hydrogen bond from MD simulations. (A) RMSD to the initial closed structure (blue) and average number of hydrogen bonds connecting L58 and E170 (red) vs simulation time. During the first 20 ps of the simulation, the closed conformation opens slightly and water molecules enter to mediate the interaction between Glu170 and Leu58. (B and C) Details of the interdomain hydrogen-bond network. The direct hydrogen bond between the amide hydrogen of Leu58 of AMPbd to O<sup>ε</sup> of Glu170 in the ATPid, as observed in the crystal structure, can be mediated by one (B) or two (C) water molecules.

principle depend on a compactification of the structure due to the presence of precipitating agents ( $\sim 2$  M ammonium sulfate<sup>11</sup>) during the crystallization procedure.

**TMAO Induced Perturbation of  $AK_{eco}$ .** Osmolytes favor compact protein states through co-solvent exclusion (alternatively denoted preferential hydration) effects.<sup>48</sup> In ribonuclease A, it has been shown that TMAO decreases the native state flexibility that was induced by the presence of guanidine hydrochloride.<sup>49</sup> Thus, TMAO can affect a protein energy landscape both at the level of folding/unfolding and native state dynamics. Therefore, in the case of  $AK_{eco}$ , TMAO may affect both the unfolding/folding and opening/closing events. These two processes were approached experimentally by monitoring effects on  $T_m$  for folding/unfolding, and of NMR chemical shifts for opening/closing. In case of  $AK_{eco}$  and E170A apo states TMAO did not introduce any significant shifts in  $T_m$  (Figure 4A,B and Table 1). The thermal stabilities of the closed Ap5A bound states were however increased around 2 °C. The result is interesting since Ap5A binds tightly to  $AK_{eco}$  ( $K_d = 0.14 \mu$ M<sup>14,50</sup>); thus, any weak nonspecific binding of TMAO to the ATP and AMP sites is occluded by the inhibitor. On the other hand, TMAO may bind to sites on the protein that is not occluded by Ap5A. It is thus possible that the stabilizing effect is due to both a co-solvent exclusion effect and weak binding of TMAO. For the opening–closing event, it has been shown with time-resolved FRET experiments that TMAO addition reduces

the distance between the side chains of residue 142 in the ATPlid and residue 203 in the CORE subdomain.<sup>51</sup> This nicely illustrates that closed conformations are favored in presence of TMAO. A  $^1\text{H}$ - $^{15}\text{N}$  HSQC spectrum of  $\text{AK}_{\text{eco}}$  in presence 0.35 M TMAO is of high quality (Supporting Information Figure 1C) and the overall chemical perturbations referenced to  $\text{AK}_{\text{eco}}$  under regular buffer conditions are relatively small (Supporting Information Figure 1D). As for E170A, the largest chemical shift perturbations occur for residues that are sensitive to ATPlid dynamics.<sup>12</sup> The structural distribution of these residues overlap with the E170A perturbation pattern (Figure 3B) which is a first indication that both E170A and osmolyte perturbations affect the same global exchange process.

**Modulation of the Open/Closed Equilibrium.** A careful inspection of the  $^1\text{H}$ - $^{15}\text{N}$  HSQC spectra of apo wild-type, apo wild-type with 0.35 M TMAO and apo E170A shows that, for several residues, the chemical shifts of these three fall onto a straight line (Figure 6A,B). This behavior indicates that the chemical shift perturbations in both hydrogen-bond and TMAO perturbed  $\text{AK}_{\text{eco}}$  are probing the same global exchange process. Similar linear trends that report on one global process have been observed in several other systems.<sup>12,29,52</sup> Since FRET experiments have shown that TMAO affects the open/closed equilibrium by stabilizing closed conformations,<sup>51</sup> we conclude that both the hydrogen bond and TMAO perturbations affect the open/closed equilibrium. In all cases, the chemical shifts of apo  $\text{AK}_{\text{eco}}$  appear in-between those of the two perturbed states. The linear response is fitted globally for the 27 residues that follow this pattern in Figure 6C. The linear response to both mutational and osmolyte driven perturbation is further substantiating that both perturbations affect the same global exchange process.

The relative change in populations of the closed state in hydrogen-bond perturbed and osmolyte perturbed  $\text{AK}_{\text{eco}}$  referenced to wild-type  $\text{AK}_{\text{eco}}$  under regular buffer conditions can be estimated from the global analysis of chemical shifts in Figure 6C. The slope of the linear correlation ( $\delta y/\delta x = 0.45$ ) corresponds to average chemical shift changes referenced according to:  $\delta y$  equals the chemical shift changes between  $\text{AK}_{\text{eco}}$  and E170A, whereas  $\delta x$  equals the chemical shift changes between 0.35 M TMAO and E170A. These chemical shift changes place the three states on the open to closed reaction coordinate; it is however not possible to extract a quantitative measure on the absolute positions on the reaction coordinate since the chemical shifts of the open and closed states in absence of substrate are presently inaccessible. Removal of the E170/L58 hydrogen bond shifts the equilibrium toward the open state, whereas TMAO addition shifts the equilibrium toward the closed state. Since apo  $\text{AK}_{\text{eco}}$  peaks always appear in-between the E170A and TMAO peaks, the linear response shows that apo  $\text{AK}_{\text{eco}}$  chemical shifts are linear combinations of chemical shifts in open and closed states. The global chemical shift correlation analysis was based upon visual inspection of NMR spectra. Chemical shift projection analysis<sup>53</sup> is an alternative approach to identify correlations between chemical shifts. We applied this approach to our data set and defined an "activation" vector from E170A toward  $\text{AK}_{\text{eco}}$  with 0.35 M TMAO (i.e., along the open to closed reaction trajectory, see Supporting Information Figure S3 for an illustration of the vector) and computed the projection angle (reported as  $\cos(\theta)$ ) and amplitude ( $X$ ) of  $\text{AK}_{\text{eco}}$  chemical shifts on this vector. The resulting projection angles and amplitudes are shown in Supporting Information Figure S4. The average

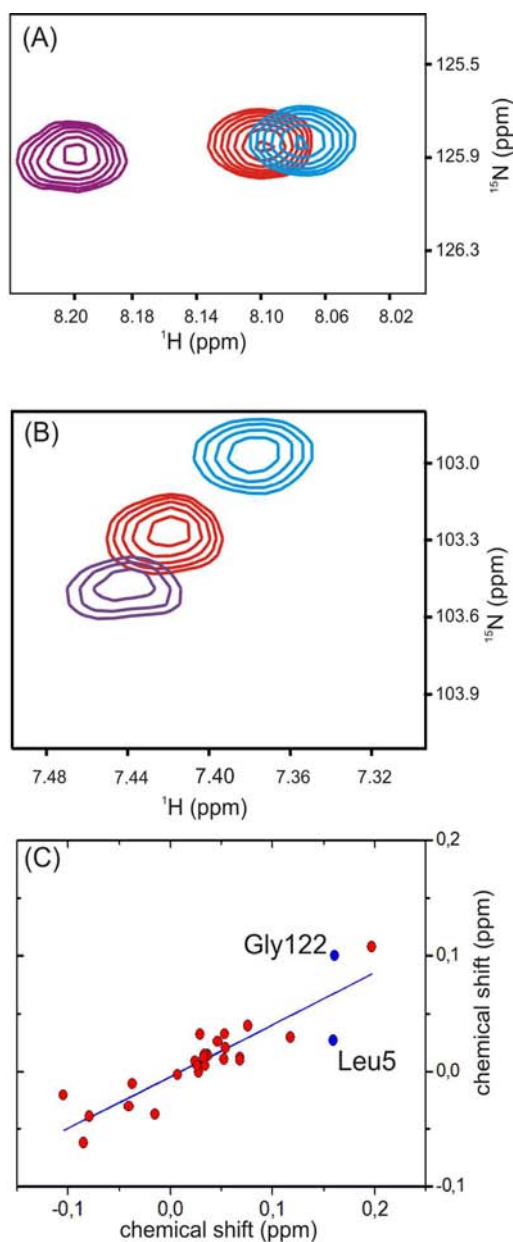


**Figure 6.** Detection and perturbation of the open/closed equilibrium in apo  $\text{AK}_{\text{eco}}$ . (A and B) Expansions of  $^1\text{H}$ - $^{15}\text{N}$  HSQC spectra of apo  $\text{AK}_{\text{eco}}$  (red contours), apo  $\text{AK}_{\text{eco}}$  in presence of 0.35 M TMAO (purple contours) and apo E170A (blue contours). Residues Leu5 and Gly122 are shown in (A) and (B), respectively. (C) Global correlation of the 27 chemical shifts that fall onto a straight line in the three states defined in (A) and (B). The x-axis corresponds to the difference in chemical shifts between E170A and  $\text{AK}_{\text{eco}}$  with 0.35 M TMAO, whereas the y-axis corresponds to the difference in chemical shifts between  $\text{AK}_{\text{eco}}$  and E170A. Chemical shifts are weighted according to  $\delta\omega = 0.2 \cdot \delta\omega^{15}\text{N} + \delta\omega^1\text{H}$  (ppm)<sup>12</sup> and the slope of the correlation is equal to 0.45. Residues Leu5 and Gly122 are indicated in blue.

projection amplitude for residues with  $\cos \theta > 0.9$  is equal to 0.53 which is strikingly similar to the result from the linear correlation analysis (0.45). The majority of analyzed residues place the three states in the same order as deduced from the linear correlation analysis. Overall, both methods identify very similar sets of residues as sensitive markers of the opening/closing reaction (Supporting Information Figure S5), even though the projection analysis identified a few additional

residues. Thus, the projection analysis reinforces the conclusion that the conformational state of  $AK_{\text{eco}}$  is between those of E170A and  $AK_{\text{eco}}$  with 0.35 M TMAO on the open to closed reaction trajectory.

These results from both the linear correlation and projection analysis suggest that  $AK_{\text{eco}}$  samples the fully closed conformation in absence of substrate and, in addition, that the E170/L58 hydrogen bond is formed and broken during the exchange between open and closed states. This finding is in good agreement with previous conclusions from single-molecule experiments where closed states were inferred from the experimental data in substrate free  $AK_{\text{eco}}$ .<sup>6,17</sup> We find it notable that perturbations driven by completely different physical mechanisms (mutation vs osmolyte) affect the same conformational exchange process in a protein albeit in different directions.

**Catalytic Activities in Response to Mutational/Osmolyte Perturbation.** Next we asked if the mutational and osmolyte induced perturbation of the open/closed equilibrium affects the catalytic properties of  $AK_{\text{eco}}$ . On the basis of the chemical shift analysis, the populations of the closed states are decreased and increased in the hydrogen bond and TMAO perturbations, respectively. With a reaction coordinate defined as the trajectory from open to closed conformations, the three can be placed in the following order: E170A,  $AK_{\text{eco}}$ , and  $AK_{\text{eco}}$  in presence of 0.35 M TMAO. The enzymatic activities of E170A and osmolyte perturbed  $AK_{\text{eco}}$  were quantified with a coupled ATP:ase assay in the direction of ADP formation<sup>31</sup> and benchmarked against the wild-type under regular buffer conditions (Figure 7 and Table 2). All variants

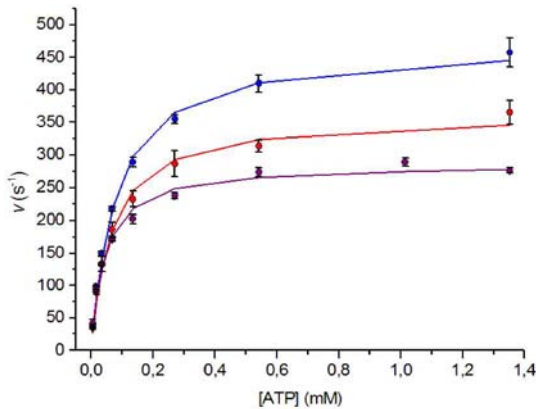


**Figure 7.** The magnitude of the open/closed equilibrium affects enzyme kinetics. Enzymatic turnover (scaled with the protein concentration), derived from a coupled ATP:ase assay with ATP as variable substrate and AMP constant at 300  $\mu\text{M}$ , is shown together with fits to Michaelis–Menten kinetics (solid lines) for  $AK_{\text{eco}}$  (red),  $AK_{\text{eco}}$  with 0.35 M TMAO (purple), and E170A (blue). Error bars are derived from triplicate measurements.

**Table 2. Enzymatic Parameters of Wild-Type and Perturbed  $AK_{\text{eco}}$**

	$k_{\text{cat}}$ ( $\text{s}^{-1}$ )	$K_{\text{M}}$ ( $\mu\text{M}$ )	$k_{\text{cat}}/K_{\text{M}}$ ( $\text{s}^{-1} \mu\text{M}^{-1}$ )
Wild-type	$360 \pm 10$	$63 \pm 7$	$5.7 \pm 0.7$
E170A	$470 \pm 10$	$78 \pm 6$	$6.0 \pm 0.5$
0.35 M TMAO	$286 \pm 7$	$42 \pm 5$	$6.8 \pm 0.8$

display Michaelis–Menten kinetics and  $k_{\text{cat}}$  and  $K_{\text{M}}$  values were quantified by fitting initial reaction velocities to the Michaelis–

Menten equation.<sup>54</sup> For the E170A perturbation (decreased closed population), we observe a 30% increase in the maximum turnover rate, and for the osmolyte perturbation (increased closed population), we observe a 20% decrease in the maximum turnover rate.

In Figure 8, the catalytic parameters of the three scenarios are plotted against relative positions on the open to closed reaction

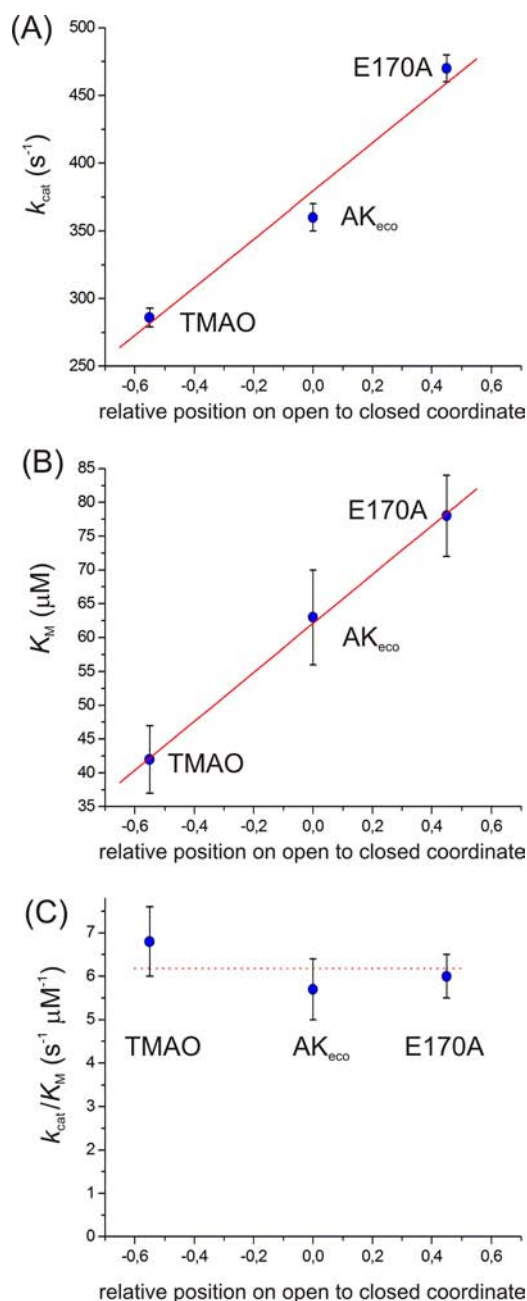


**Figure 8.** Correlation between enzymatic parameters and chemical shifts. The relative position on the open to closed reaction coordinate is from the slope (0.45) in Figure 6C. The  $x$ -axis should be interpreted as: if the distance from E170A to  $AK_{\text{eco}}$  in the direction of the open state is 0.45, then the distance from  $AK_{\text{eco}}$  with TMAO to  $AK_{\text{eco}}$  in the direction of the closed state equals “0.55”. The best fitted straight lines are shown as solid red lines. (A) Correlation between  $k_{\text{cat}}$  and chemical shifts. (B) Correlation between  $K_{\text{M}}$  and chemical shifts. (C) Correlation between  $k_{\text{cat}}/K_{\text{M}}$  and chemical shifts. The average  $k_{\text{cat}}/K_{\text{M}}$  value is indicated as a dotted line.

coordinate. It should be noted that the relative positions cannot be scaled to obtain a quantitative number since the chemical shifts of the “true” open and closed substrate free states are currently inaccessible. It thus seems possible to rationally tune the maximum turnover rate in  $AK_{\text{eco}}$  simply by stabilizing or destabilizing the closed state relative to the open state.

We also observe a strong linear correlation between the  $K_M$  values and the population changes in the perturbed  $AK_{\text{eco}}$  states (Figure 8B). The  $K_M$  values in E170A and TMAO perturbations are 78 and 42  $\mu\text{M}$ , respectively. These values should be compared to a  $K_M$  of 63  $\mu\text{M}$  for  $AK_{\text{eco}}$  under regular buffer conditions. These observations can be rationalized by the fact that nucleotide binding affinity scale with the closed populations according to Figure 1D (and acknowledging that  $K_M$  is reflecting a nominal ATP binding affinity).

However, the  $K_M$  value can only be treated as a nominal binding affinity. Thus, it is important to benchmark the ATP binding affinities for the E170A and TMAO perturbations against the  $K_d$  of the wild-type (53  $\mu\text{M}$ <sup>12</sup>). To this end, we used NMR titrations to quantify the  $K_d$  values for ATP binding for E170A in regular buffer and wild-type  $AK_{\text{eco}}$  in presence of 0.35 M TMAO (Figure 9). Note, that the  $K_d$  values should be

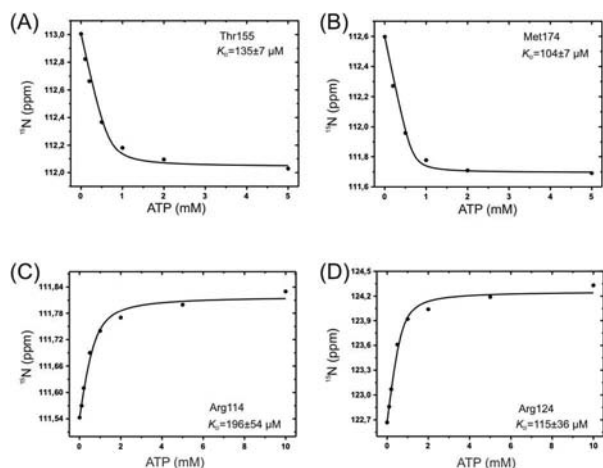


**Figure 9.** NMR detected ATP binding experiments. (A and B) Residue specific ATP binding isotherms for wild-type  $AK_{\text{eco}}$  with 0.35 M TMAO. (C and D) Residue specific ATP binding isotherms for E170A. The solid lines correspond to fits to one-site binding models.

interpreted as “apparent”  $K_d$  values since all substrate bound states will contribute to the binding affinity. The  $K_d$  values were determined for assigned residues in the ATPlid (defined as residues 113–176) and the reported values are averages over all analyzed residues. For E170A, we observe a  $K_d$  value of  $150 \pm 44 \mu\text{M}$ ; thus, the hydrogen bond perturbation decreases the ATP binding affinity which is reflected in an increased  $K_M$  value. This result is consistent with a conformational selection model for ATP binding since the wild-type that is more shifted toward the closed state (compared to E170A) binds ATP with higher affinity. In case of  $AK_{\text{eco}}$  with 0.35 M TMAO, we observe a  $K_d$  value of  $150 \pm 16 \mu\text{M}$ ; thus, the decreased  $K_M$  value cannot be rationalized with an improved ATP binding activity. In principle, the decreased catalytic activity in presence of 0.35 M TMAO can depend on weak binding of TMAO to  $AK_{\text{eco}}$ , and that TMAO is acting as a noncompetitive inhibitor (which would explain the reduced ATP binding affinity). This explanation cannot be ruled out, but it is clear that the chemical shift perturbation pattern driven by 0.35 M TMAO is not

consistent with a small molecule binding to the enzyme for three reasons: (1) the chemical shift pattern is overlapping with that of ATP binding (Figure 3B,C), (2) the conformational equilibrium is shifted toward the closed state with 0.35 M TMAO (Figure 6C), (3) the  $T_m$  of both substrate free  $AK_{\text{eco}}$  and E170A is not significantly perturbed by 0.35 M TMAO which is expected for a binding event. Finally, FRET experiments have shown that TMAO favors closed  $AK_{\text{eco}}$  states.<sup>51</sup> It can also not be ruled out that the microscopic mechanisms of  $AK_{\text{eco}}$  catalysis are altered in the presence of TMAO. In summary, for the E170A modification, the perturbation of  $k_{\text{cat}}$  and  $K_M$  values is dependent on a population shift toward the open state of this variant. For the situation of  $AK_{\text{eco}}$  with 0.35 M TMAO, the effects on  $k_{\text{cat}}$  and  $K_M$  are likely a result of both a shift toward the closed state and weak residual binding of TMAO to the enzyme.

## CONCLUSIONS

Here, we have utilized the full resolution capacity of NMR spectroscopy to study an enzyme at the level of an individual atom ( $H^N$  of Leu58). Moreover, we have shown that hydrogen bonding to this atom (which is distant from the active site) directly influences the catalytic properties of  $AK_{\text{eco}}$ . MD simulations indicate that water molecules enable breathing within the closed  $AK_{\text{eco}}$  ensemble mediating the hydrogen bond between Leu58 and Glu170. Since the hydrogen bond affects the catalytic properties of  $AK_{\text{eco}}$ , the involvement of water in mediating this bond suggests that the water molecules are directly coupled to  $AK_{\text{eco}}$  activity. Similarly, structural waters embedded in cavities have been observed in many proteins.<sup>55</sup> These water molecules often make hydrogen bonds to otherwise “naked” hydrogen bond donor and acceptor groups and can, as a consequence, increase protein stability.<sup>55,56</sup> For  $AK_{\text{eco}}$  and also other kinases, it is important to remove water molecules from the active site to prevent nonproductive hydrolysis of ATP. In  $AK_{\text{eco}}$ , this is accomplished with a large-scale conformational change that together with substrate binding will generate a dry active site void of water. In light of our findings, it seems that structural water molecules not only can influence the stability of proteins, be directly involved in chemical mechanisms,<sup>13</sup> or cause unwanted side-reactions in enzymes, but can also take an active part during conformational changes. Removal of the Leu58 hydrogen bond increases the catalytic parameters  $k_{\text{cat}}$  and  $K_M$  by decreasing the population of the closed and active  $AK_{\text{eco}}$  conformation. An osmolyte perturbation acts to increase the same population and results in decreased  $k_{\text{cat}}$  and  $K_M$  values. It is however important to note that the TMAO effect on the catalytic parameters likely is dependent on both a shift of the open-closed equilibrium and weak nonspecific TMAO binding to  $AK_{\text{eco}}$ . We<sup>5</sup> and others<sup>6</sup> have previously shown that  $AK_{\text{eco}}$  catalysis is rate-limited by the opening of the substrate binding subdomains in the presence of bound nucleotides. Hence, destabilization of the closed state is expected to increase the rate of  $AK_{\text{eco}}$  catalysis. The kinetics of subdomain opening can alternatively be expressed as the reciprocal of the lifetime of the closed conformation ( $= 1/\tau_c$ ). In this study, we show a strong link between the population of the closed  $AK_{\text{eco}}$  state and catalytic activity. In light of the relatively small changes in catalytic activity between the wild-type enzyme and the perturbations employed here, it is likely that the rate-limiting step is subdomain opening also in the perturbations. Under this assumption, the population changes are linked to increased and decreased lifetimes of the closed

state in the osmolyte and hydrogen bond perturbations, respectively. Therefore (under the assumption stated above), our previous observation that  $AK_{\text{eco}}$  turnover is rate-limited by conformational dynamics is reinforced and taken to the level where “rational” modulation of the open/closed equilibrium results in catalytic parameters that change in a direction that is predictable from the catalytic model. We find it remarkable that perturbations driven by either hydrogen bond removal or osmolyte addition affect the same conformational exchange process in  $AK_{\text{eco}}$ . The hydrogen bond and osmolyte perturbations both affect closed versus open populations albeit in different directions. This observation suggests that TMAO perturbations of NMR chemical shifts may open a new avenue for identification and quantification of conformational dynamics in proteins. Both  $k_{\text{cat}}$  and  $K_M$  scale linearly in response to perturbation of the open/closed equilibrium, which can be nicely illustrated by plotting both  $k_{\text{cat}}$  and  $K_M$  versus relative chemical shifts in the wild-type and perturbed states (Figure 8A,B). It has been shown previously that a conformational equilibrium within a membrane associated protein substrate affects the rate of phosphorylation by cAMP-dependent protein kinase A.<sup>57</sup> Thus, it appears that dynamics of both substrates and enzymes needs to be considered in order to picture a complete “native state” free energy landscape during catalysis. A pre-existing equilibrium (i.e., in absence of substrate), corresponding to the opening and closure of  $AK_{\text{eco}}$  was inferred from the observation of linear chemical shift trends in  $^1\text{H}$ – $^{15}\text{N}$  HSQC NMR experiments. Notably, activity measurements show that the magnitude of the pre-existing equilibrium directly influences the catalytic properties of the enzyme. There exist many reasons to develop enzymes with increased catalytic activity; our results show that in the case of enzymes where conformational dynamics is rate-limiting for catalysis in ways similar to  $AK_{\text{eco}}$ , an increase (or decrease) of the catalytic activity is linked to a proportional change of the Michaelis constant. In analogy to enthalpy–entropy compensation<sup>58,59</sup> observed for weak interactions in for instance protein folding and ligand binding,<sup>60</sup> such systems display  $k_{\text{cat}}-K_M$  compensation upon perturbation (Figure 8C). Similar observations of  $k_{\text{cat}}-K_M$  compensation has been observed previously for the oxidative repair enzyme AlkB.<sup>61</sup> The  $k_{\text{cat}}-K_M$  compensation also has significance for the evolution of enzymes where the most important catalytic parameter for an enzyme under cellular conditions is the specificity constant,  $k_{\text{cat}}/K_M$ . For enzymes that display a similar co-variation in  $k_{\text{cat}}$  and  $K_M$ , there exist many alternative routes to obtain a  $k_{\text{cat}}/K_M$  value that is optimal for function. For example, in the  $AK_{\text{eco}}$  case, removal of one interdomain hydrogen bond (that affects both  $k_{\text{cat}}$  and  $K_M$ ) generates an enzyme with a specificity constant that is silent to the perturbation. Thus, it appears that  $AK_{\text{eco}}$  has evolved to be intrinsically robust with respect to the  $k_{\text{cat}}/K_M$  ratio. As a concluding remark, our study highlights the tight and complex interplay between native state enzyme dynamics and catalytic properties.

**Abbreviations.**  $AK_{\text{eco}}$ , Adenylate kinase from *Escherichia coli*; E170A,  $AK_{\text{eco}}$  E170A mutation; HSQC, heteronuclear single quantum coherence; NMR, Nuclear magnetic resonance; TMAO, trimethylamine *N*-oxide.

## ■ ASSOCIATED CONTENT

### ■ Supporting Information

Supporting Information Figure S1,  $^1\text{H}$ – $^{15}\text{N}$  HSQC spectra of the three variants  $AK_{\text{eco}}$ , E170A and  $AK_{\text{eco}}$  with 0.35 M TMAO;

Supporting Information Figure S2, RMSD and analysis of L58/E170 hydrogen bonds for two MD simulations; Supporting Information Figures S3–S5, chemical shift projection analysis; hydrogen exchange data for Leu58 in presence of Ap5A and a detailed explanation of  $K_{\text{conf}}$ ,  $^1\text{H}$  and  $^{15}\text{N}$  chemical shifts have been deposited at the BMRB with the following accession codes: 18683 (wild-type  $AK_{\text{eco}}$ ), 18686 (E170A), 18687 ( $AK_{\text{eco}}$  with 0.35 M TMAO). This material is available free of charge via the Internet at <http://pubs.acs.org>.

## ■ AUTHOR INFORMATION

### Corresponding Author

[magnus.wolf-watz@chem.umu.se](mailto:magnus.wolf-watz@chem.umu.se)

### Notes

The authors declare no competing financial interest.

## ■ ACKNOWLEDGMENTS

This research was financially supported by the Swedish Research Council (Grant Number 621-2010-5247), and an Umeå University “Young Researcher Award” to M.W.-W. A.S. recognizes support by the Impuls- und Vernetzungsfonds of the Helmholtz-Association and the SimLab NanoMicro (SCC, Karlsruhe Institute of Technology). The MD simulations were performed using the resources of bwGRiD.

## ■ REFERENCES

- (1) Radzicka, A.; Wolfenden, R. *Science* **1995**, *267*, 90.
- (2) Boehr, D. D.; McElheny, D.; Dyson, H. J.; Wright, P. E. *Science* **2006**, *313*, 1638.
- (3) Beach, H.; Cole, R.; Gill, M. L.; Loria, J. P. *J. Am. Chem. Soc.* **2005**, *127*, 9167.
- (4) Eisenmesser, E. Z.; Millet, O.; Labeikovsky, W.; Korzhnev, D. M.; Wolf-Watz, M.; Bosco, D. A.; Skalicky, J. J.; Kay, L. E.; Kern, D. *Nature* **2005**, *438*, 117.
- (5) Wolf-Watz, M.; Thai, V.; Henzler-Wildman, K.; Hadjipavlou, G.; Eisenmesser, E. Z.; Kern, D. *Nat. Struct. Mol. Biol.* **2004**, *11*, 945.
- (6) Hanson, J. A.; Duderstadt, K.; Watkins, L. P.; Bhattacharyya, S.; Brokaw, J.; Chu, J. W.; Yang, H. *Proc. Natl. Acad. Sci. U.S.A.* **2007**, *104*, 18055.
- (7) Lange, O. F.; Lakomek, N. A.; Fares, C.; Schroder, G. F.; Walter, K. F.; Becker, S.; Meiler, J.; Grubmuller, H.; Griesinger, C.; de Groot, B. L. *Science* **2008**, *320*, 1471.
- (8) Rundqvist, L.; Ådén, J.; Sparrman, T.; Wallgren, M.; Olsson, U.; Wolf-Watz, M. *Biochemistry* **2009**, *48*, 1911.
- (9) Bae, E.; Phillips, G. N., Jr. *Proc. Natl. Acad. Sci. U.S.A.* **2006**, *103*, 2132.
- (10) Müller, C. W.; Schlauderer, G. J.; Reinstein, J.; Schulz, G. E. *Structure* **1996**, *4*, 147.
- (11) Müller, C. W.; Schulz, G. E. *J. Mol. Biol.* **1992**, *224*, 159.
- (12) Ådén, J.; Wolf-Watz, M. *J. Am. Chem. Soc.* **2007**, *129*, 14003.
- (13) Fersht, A. *Structure and mechanism in protein science. A guide to enzyme catalysis and protein folding*, W.H. Freeman and Company: New York, 2000.
- (14) Olsson, U.; Wolf-Watz, M. *Nat. Commun.* **2010**, DOI: 10.1038/ncomms1106.
- (15) Whitford, P. C.; Miyashita, O.; Levy, Y.; Onuchic, J. N. *J. Mol. Biol.* **2007**, *366*, 1661.
- (16) Koradi, R.; Billeter, M.; Wüthrich, K. *J. Mol. Graphics* **1996**, *14*, 51.
- (17) Henzler-Wildman, K. A.; Thai, V.; Lei, M.; Ott, M.; Wolf-Watz, M.; Fenn, T.; Pozharski, E.; Wilson, M. A.; Petsko, G. A.; Karplus, M.; Hübner, C. G.; Kern, D. *Nature* **2007**, *450*, 838.
- (18) Gambin, Y.; Schug, A.; Lemke, E. A.; Lavinder, J. J.; Ferreon, A. C. M.; Magliery, T. J.; Onuchic, J. N.; Deniz, A. A. *Proc. Natl. Acad. Sci. U.S.A.* **2009**, *106*, 10153.

- (19) Loria, J. P.; Rance, M.; Palmer, A. G. *J. Am. Chem. Soc.* **1999**, *121*, 2331.
- (20) Tollinger, M.; Skrynnikov, N. R.; Mulder, F. A.; Forman-Kay, J. D.; Kay, L. E. *J. Am. Chem. Soc.* **2001**, *123*, 11341.
- (21) Bouvignies, G.; Vallurupalli, P.; Hansen, D. F.; Correia, B. E.; Lange, O.; Bah, A.; Vernon, R. M.; Dahlquist, F. W.; Baker, D.; Kay, L. E. *Nature* **2011**, *477*, 111.
- (22) Cavalli, A.; Salvatella, X.; Dobson, C. M.; Vendruscolo, M. *Proc. Natl. Acad. Sci. U.S.A.* **2007**, *104*, 9615.
- (23) Shen, Y.; Lange, O.; Delaglio, F.; Rossi, P.; Aramini, J. M.; Liu, G.; Eletsky, A.; Wu, Y.; Singarapu, K. K.; Lemak, A.; Ignatchenko, A.; Arrowsmith, C. H.; Szyperski, T.; Montelione, G. T.; Baker, D.; Bax, A. *Proc. Natl. Acad. Sci. U.S.A.* **2008**, *105*, 4685.
- (24) Sborgi, L.; Verma, A.; Munoz, V.; de Alba, E. *PLoS One* **2011**, *6*.
- (25) Berjanskii, M. V.; Wishart, D. S. *J. Am. Chem. Soc.* **2005**, *127*, 14970.
- (26) Berjanskii, M. V.; Wishart, D. S. *Nucleic Acids Res.* **2007**, *35*, W531.
- (27) Berjanskii, M. V.; Wishart, D. S. *J. Biomol. NMR* **2008**, *40*, 31.
- (28) Berjanskii, M.; Wishart, D. S. *Nat. Protoc.* **2006**, *1*, 683.
- (29) Selvaratnam, R.; Chowdhury, S.; VanSchouwen, B.; Melacini, G. *Proc. Natl. Acad. Sci. U.S.A.* **2011**, *108*, 6133.
- (30) Consalvi, V.; Chiaraluce, R.; Giangiacomo, L.; Scandurra, R.; Christova, P.; Karshikoff, A.; Knapp, S.; Ladenstein, R. *Protein Eng.* **2000**, *13*, 501.
- (31) Rhoads, D. G.; Lowenstein, J. M. *J. Biol. Chem.* **1968**, *243*, 3963.
- (32) Delaglio, F.; Grzesiek, S.; Vuister, G. W.; Zhu, G.; Pfeifer, J.; Bax, A. *J. Biomol. NMR* **1995**, *6*, 277.
- (33) Helgstrand, M.; Kraulis, P.; Allard, P.; Härd, T. *J. Biomol. NMR* **2000**, *18*, 329.
- (34) Lindorff-Larsen, K.; Piana, S.; Palmo, K.; Maragakis, P.; Klepeis, J. L.; Dror, R. O.; Shaw, D. E. *Proteins: Struct., Funct., Bioinf.* **2010**, *78*, 1950.
- (35) Jorgensen, W. L.; Chandrasekhar, J.; Madura, J. D.; Impey, R. W.; Klein, M. L. *J. Chem. Phys.* **1983**, *79*, 926.
- (36) Van der Spoel, D.; Lindahl, E.; Hess, B.; Groenhof, G.; Mark, A. E.; Berendsen, H. J. C. *J. Comput. Chem.* **2005**, *26*, 1701.
- (37) Kabsch, W.; Sander, C. *Biopolymers* **1983**, *22*, 2577.
- (38) Englander, S. W.; Mayne, L.; Bai, Y.; Sosnick, T. R. *Protein Sci.* **1997**, *6*, 1101.
- (39) Englander, S. W.; Kallenbach, N. R. *Q. Rev. Biophys.* **1984**, *16*, 521.
- (40) Pontiggia, F.; Zen, A.; Micheletti, C. *Biophys. J.* **2008**, *95*, 5901.
- (41) Brokaw, J. B.; Chu, J. W. *Biophys. J.* **2010**, *99*, 3420.
- (42) Snow, C.; Qi, G. Y.; Hayward, S. *Proteins: Struct., Funct., Bioinf.* **2007**, *67*, 325.
- (43) Potoyan, D. A.; Zhuravlev, P. I.; Papoian, G. A. *J. Phys. Chem. B* **2012**, *116*, 1709.
- (44) Shehu, A.; Kavraki, L. E.; Clementi, C. *Proteins: Struct., Funct., Bioinf.* **2009**, *76*, 837.
- (45) Nygaard, R.; Valentin-Hansen, L.; Mokrosinski, J.; Frimurer, T. M.; Schwartz, T. W. *J. Biol. Chem.* **2010**, *285*, 19625.
- (46) Levy, Y.; Onuchic, J. N. *Annu. Rev. Biophys. Biomol. Struct.* **2006**, *35*, 389.
- (47) Cerutti, D. S.; Freddolino, P. L.; Duke, R. E., Jr.; Case, D. A. *J. Phys. Chem. B* **2010**, *114*, 12811.
- (48) Lin, T. Y.; Timasheff, S. N. *Biochemistry* **1994**, *33*, 12695.
- (49) Doan-Nguyen, V.; Loria, J. P. *Protein Sci.* **2007**, *16*, 20.
- (50) Schrank, T. P.; Bolen, D. W.; Hilser, V. J. *Proc. Natl. Acad. Sci. U.S.A.* **2009**, *106*, 16984.
- (51) Nagarajan, S.; Amir, D.; Grupi, A.; Goldenberg, D. P.; Minton, A. P.; Haas, E. *Biophys. J.* **2011**, *100*, 2991.
- (52) Volkman, B. F.; Lipson, D.; Wemmer, D. E.; Kern, D. *Science* **2001**, *291*, 2429.
- (53) Selvaratnam, R.; VanSchouwen, B.; Fogolari, F.; Mazhab-Jafari, M. T.; Das, R.; Melacini, G. *Biophys. J.* **2012**, *102*, 630.
- (54) Michaelis, L.; Menten, M. L. *Biochem. Z.* **1913**, *49*, 333.
- (55) Park, S.; Saven, J. G. *Proteins: Struct., Funct., Bioinf.* **2005**, *60*, 450.
- (56) Takano, K.; Yamagata, Y.; Yutani, K. *Protein Eng.* **2003**, *16*, 5.
- (57) Masterson, L. R.; Yu, T.; Shi, L.; Wang, Y.; Gustavsson, M.; Mueller, M. M.; Veglia, G. *J. Mol. Biol.* **2011**, *412*, 155.
- (58) Liu, L.; Guo, Q. X. *Chem. Rev.* **2001**, *101*, 673.
- (59) Dunitz, J. D. *Chem. Biol.* **1995**, *2*, 709.
- (60) Schug, A.; Onuchic, J. N. *Curr. Opin. Pharmacol.* **2010**, *10*, 709.
- (61) Yu, B.; Hunt, J. F. *Proc. Natl. Acad. Sci. U.S.A.* **2009**, *106*, 14315.